CO2 to CO: Photo- and electrocatalytic conversion based on Re(I) Bis-Arene Frameworks: synergisms between catalytic subunits

Hernández-Valdés, Daniel ; Fernández-Terán, Ricardo ; Probst, Benjamin ; Spingler, Bernhard ; Alberto, Roger

Abstract: Reduction of CO2 to CO and H2O is a two electron/two proton process. For this process, multinuclear complexes offer advantages by concentrating reduction equivalents more efficiently than mononuclear systems. We present novel complexes with [Re(6-C6H6)2]+ as scaffold conjugated to one or two catalytically active [Ru(dmbpy)(CO)2Cl2] subunits (dmbpy=5,5 -dimethyl-2,2 -bipyridine). The [Re(6-C6H6)2]+ scaffold was chosen due to its very high photo- and chemical stability, as well as the multiple degrees of freedom it offers for any conjugated functionalities. High efficiency and selectivity for the reduction of CO2 to CO (over H2 or HCOOH) is reported. TONs and TOFs were found to be comparable or higher than for the catalyst subunit without the rhenium framework. Cooperativity in photo- and electrocatalysis is observed for the complex comprising two catalytic subunits. The synergistic communication between the two catalytic subunits is responsible for the observed enhancement in both photo- and electrocatalytic performance. Confirmation of electronic communication between the two [Ru(dmbpy)(CO)2Cl2] subunits as well as the elucidation of a possible mechanism was supported by electrochemistry, IR-spectroelectrochemistry and DFT studies.

DOI: https://doi.org/10.1002/hlca.202000147

CO_2 to CO: Photo- and Electrocatalytic Conversion Based on Re(I) Bis-Arene Frameworks: Synergisms Between Catalytic Subunits

Daniel Hernández-Valdés,[a] Ricardo Fernández-Terán,[a] Benjamin Probst,[a] Bernhard Spingler,[a] and Roger Alberto*[a]

[a] Department of Chemistry, University of Zurich
Winterthurerstrasse 190, CH-8057, Zurich, Switzerland, e-mail: ariel@chem.uzh.ch

Dedicated to Prof. *Michael Grätzel's* 75th birthday

Reduction of CO_2 to CO and H_2O is a two electron/two proton process. For this process, multinuclear complexes offer advantages by concentrating reduction equivalents more efficiently than mononuclear systems. We present novel complexes with $[Re(\eta^6\text{-}C_6H_6)_2]^+$ as scaffold conjugated to one or two catalytically active [Ru(dmbpy)$(CO)_2Cl_2$] subunits (dmbpy = 5,5′-dimethyl-2,2′-bipyridine). The $[Re(\eta^6\text{-}C_6H_6)_2]^+$ scaffold was chosen due to its very high photo- and chemical stability, as well as the multiple degrees of freedom it offers for any conjugated functionalities. High efficiency and selectivity for the reduction of CO_2 to CO (over H_2 or HCOOH) is reported. TONs and TOFs were found to be comparable or higher than for the catalyst subunit without the rhenium framework. Cooperativity in photo- and electrocatalysis is observed for the complex comprising two catalytic subunits. The synergistic communication between the two catalytic subunits is responsible for the observed enhancement in both photo- and electrocatalytic performance. Confirmation of electronic communication between the two [Ru(dmbpy)$(CO)_2Cl_2$] subunits as well as the elucidation of a possible mechanism was supported by electrochemistry, IR-spectroelectrochemistry and DFT studies.

Keywords: CO_2 reduction, photocatalysis, electrocatalysis, rhenium bis(arene), synergism, photochemistry, electrochemistry.

Introduction

The increase in energy demand and the challenge of how to answer to this requirement in the near future is a central issue in today's science and society. In addition, climate change is an accepted scenario and therefore, finding fossil-fuel-independent energy sources is urgent. Sunlight is the ultimate source of energy that has to be used in future.[1,2] Inspired by the concept of photosynthesis, where solar energy is stored for longer term use in the form of chemical bonds, CO_2 could be the primary source of carbon for the new generation of environmentally friendly fuels.[3–7]

Converting CO_2 selectively and efficiently into valuable chemical compounds using solar energy has attracted significant research interest since the 80's, when it was shown that photo- and electrocatalytic CO_2 reduction with Re-bipyridine, Co or Ni cyclam and porphyrin complexes, was possible.[8–10] Since then, different molecular approaches for CO_2 reduction have been investigated with for example transition metal-based molecular catalysts.[4,11–18] The one-electron reduction of CO_2 to CO_2^- is thermodynamically challenging as it requires very negative potentials (−1.9 V *vs.* SHE). The anion-radical CO_2^- is a very strong reductant, being easily reoxidized to CO_2. Therefore, multi-electronic CO_2 reductions are desired. The search for catalysts that can drive these reactions remains an important and active area of research.[19–21] The two-electron reduction of CO_2 produces CO or HCOOH depending on many factors, such as catalyst

Supporting information for this article is available on the WWW under https://doi.org/10.1002/hlca.202000147

design, concentration, solvent, pH, *etc.*[4,11,18,22] Additionally, in aqueous medium, the reduction of CO_2 to CO or HCOOH competes with the reduction of protons to H_2, which is thermodynamically more favorable. Therefore, finding catalysts that are highly efficient but at the same time selective to one of these products is essential.

Although the majority of examples found in literature as CO_2 reduction catalysts are mononuclear complexes, polynuclear complexes could be beneficial since the different catalytic subunits could potentially cooperate with each other, thereby achieving greater efficiency in CO_2 reduction. It has been shown that the combination of more than one modality (for example, photosensitizer and catalyst) in supramolecular compounds improves catalytic performance.[23–27] Several reported examples show that dinuclear catalysts of Fe (III), Co(II), Ni(II), Re(I) or even Cu(II) display significantly better catalytic performance in CO_2 reduction than their mononuclear analogues.[28–37] Improvement in activity is supposed to be a result of synergistic effects between the respective subunits. Coupling two or more active complexes can be achieved by a flexible linker (alkyl chains, *etc.*) or by a more rigid scaffold, keeping the two subunits in a specific arrangement. Many purely organic compounds have been reported as linkers in the context of catalysis.[24,38–42]

In our search for new organometallic building blocks for catalysis, we recently developed a series of $[Re(\eta^6\text{-}C_6H_5\text{-}R)_2]^+$ complexes, structurally similar to ferrocene but of higher stabilities. Some systems proved to be suitable scaffolds for proton reduction catalysis.[43] Complexes of the $[Re(\eta^6\text{-arene})_2]^+$ type have been barely studied, despite being discovered about 60 years ago.[44] These sandwich complexes can be prepared along a convenient and flexible route.[45–49] They are extraordinarily stable under harsh conditions. No decomposition occurs upon heating up to 160 °C and no cleavage of the arene ligands is generally observed under light irradiation. Besides, $[Re(\eta^6\text{-arene})_2]^+$ complexes are redox stable, the oxidation ($Re^{I/II}$) only takes place at potentials higher than +1.3 V, whereas the reduction ($Re^{I/0}$) occurs at very negative potentials, usually < −2.0 V (both *vs.* Ag/AgCl). Besides its stability and in contrast to other scaffolds connecting two active moieties in a coplanar arrangement, the sandwich framework offers structural freedom and communication between the catalytic subunits (*Scheme 1*). The flexibility of the $[Re(\eta^6\text{-arene})_2]^+$ thus allows the interaction of the different subunits involved in catalysis but without interfering with each other in the individual processes.

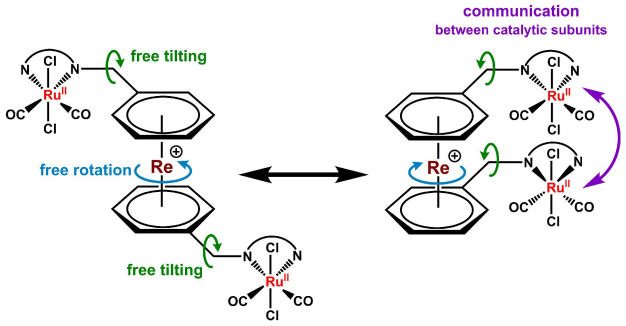

Scheme 1. Representation of degrees of freedom and communication of two catalytic subunits conjugated to a $[Re(\eta^6\text{-arene})_2]^+$ framework.

In this work, we present a supramolecular and unique architecture that selectively and efficiently reduces CO_2 to CO under photo- or electrocatalytic conditions. We describe the conjugation of one or two units of $[Ru(dmbpy)(CO)_2Cl_2]$ (dmbpy = 5,5′-dimethyl-2,2′-bipyridine) to the $[Re(\eta^6\text{-arene})_2]^+$ framework. Catalytic studies, stabilities and selectivities for CO_2 to CO reduction are shown in detail. The synergistic enhancement in catalysis between the different fragments is established and a possible mechanism behind the cooperativity is discussed.

Results and Discussion

Synthesis of Catalysts

As previously shown by our group, $[Re(\eta^6\text{-}C_6H_6)_2]^+$ is mono or bis-lithiated with $LiN(^iPr)_2$ (LDA).[43,49] The corresponding lithiated species react then with electrophiles such as C_2Cl_6 to obtain the respective chloride derivatives ($[Re(\eta^6\text{-}C_6H_5Cl)(\eta^6\text{-}C_6H_6)]^+$ (**2a**$^+$) and $[Re(\eta^6\text{-}C_6H_5Cl)_2]^+$ (**2b**$^+$) (*Scheme 2*). Complexes **2a**$^+$ and **2b**$^+$ are highly susceptible to nucleophilic attack due to the electron withdrawing effect of the Re(I) center.[43,49] Lithiation of 5,5′-dimethyl-2,2′-bipyridine (dmbpy) with LDA and subsequent substitution of Cl^- in complexes **2a**$^+$ and **2b**$^+$ leads to the formation of complexes $[Re(\eta^6\text{-}C_6H_5\text{-}C_{12}H_{11}N_2)(\eta^6\text{-}C_6H_6)]^+$ (**3a**$^+$) and $[Re(\eta^6\text{-}C_6H_5\text{-}C_{12}H_{11}N_2)_2]^+$ (**3b**$^+$) (*Scheme 2*). The complexes were separated by preparative HPLC and precipitated as PF_6^- salts in 21.4% and 12.4% yields, respectively. Single crystal structures and a full set of analytical data of both complexes confirmed their identities (*Figure 1*).

Reactions of complexes **3a**$^+$ and **3b**$^+$ with $[Ru(CO)_2Cl_2]_n$ (synthesized according to literature[50]) in methanol at room temperature resulted in the

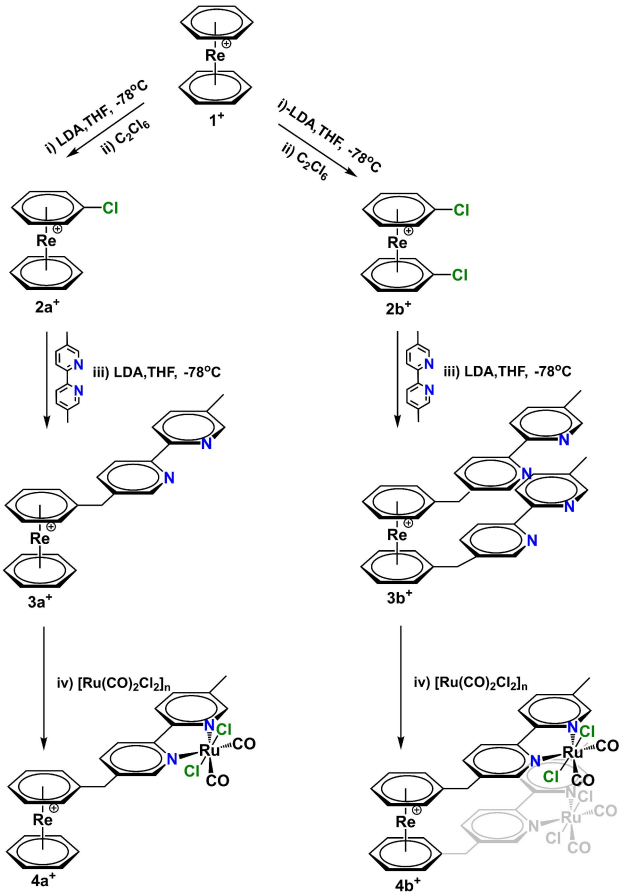

Scheme 2. Reaction scheme for the conjugation of 5,5′-dimethyl-2,2′-bipyridine to $[Re(\eta^6\text{-}C_6H_6)_2]^+$. Reaction conditions: **i)** lithiation/deprotonation 1.5–2.5 equiv. LDA, 1.5 h, −78 °C, THF. **ii)** *In situ* electrophilic attack 5 h, −78 °C, THF; electrophile: C_2Cl_6. iii) Lithiation/deprotonation of 5,5′-dimethyl-2,2′-bipyridine with 1.3 equiv. of LDA with respect to dmbpy, 1.5 h, −78 °C, THF and *in situ* nucleophilic substitution of Cl^- in complex **2a/b**$^+$. iv) Complexation, $[Ru(CO)_2Cl_2]_n$ as precursor, 1 d, r.t.

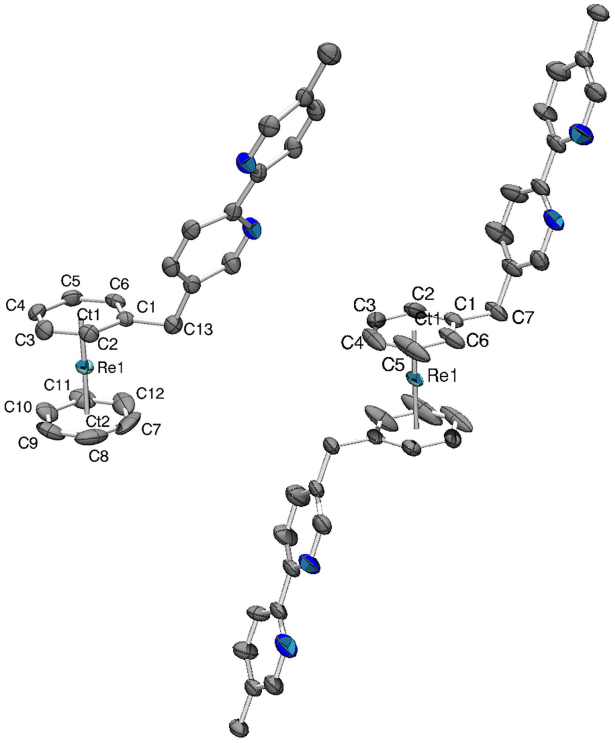

Figure 1. Displacement ellipsoid representations of cations **3a**$^+$ (left) and **[3b H]**$^{2+}$ (right). Hydrogen atoms, anions, the disordered proton at two pyridine groups of **[3b H]**$^{2+}$ and water molecules have been omitted for clarity; thermal ellipsoids represent 50 % probability. Selected bond lengths [Å] for **3a**$^+$: Re1–Centroid1 1.7207(13), Re1–Centroid2 1.727(3), Re1–C1 2.234(3), Re–C2 2.220(3), Re1–C3 2.221(3), Re1–C4 2.226(4), Re1–C5 2.229(4), Re1–C6 2.230(3), Re1–C7 2.206(6), Re1–C8 2.228(6), Re1–C9 2.227(4), Re1–C10 2.226(4), Re1–C11 2.236(4), Re1–C12 2.214(5), C1–C13 1.505(5). For **[3b H]**$^{2+}$ see *Supplementary Information.*

formation of complexes $[Re(\eta^6\text{-}C_6H_5\text{-}(Ru(dmbpy)(CO)_2Cl_2))(\eta^6\text{-}C_6H_6)]^+$ (**4a**$^+$) and $[Re(\eta^6\text{-}C_6H_5\text{-}(Ru(dmbpy)(CO)_2Cl_2))_2]^+$ (**4b**$^+$) (*Scheme 2*). The complexes were separated by preparative HPLC as TFA^- salts in 65.5 % and 26.2 % yields of isolated product, respectively. Spectroscopy and characterization by NMR and FT-IR confirmed the formation of the new products (see *Electronic Supporting Information*). Complexes **4a**$^+$ and **4b**$^+$ are electronically decoupled from the $[Re(\eta^6\text{-arene})_2]^+$ unit, and therefore, no electronic communication between the individual Ru units and the Re-center is expected. Moreover, in agreement with our previous results in this chemistry, the symmetry of all NMR spectra supports the free rotation around the rhenium axis.[43,45–49,51] Two additional Ru(II) carbonyl catalysts were prepared as reference compounds: $[Re(\eta^6\text{-}C_6H_5\text{-}(Ru(bpy)(CO)_2Cl_2)(\eta^6\text{-}C_6H_6)]^+$ (**6a**$^+$; yield of isolated product: 28.7 %), in which the bipyridyl ligand and the sandwich complex are electronically coupled (that is, without the methylene group in between them) and *trans*(Cl)-$[Ru(dmbpy)(CO)_2Cl_2]$ (**7**; yield of isolated product: 53.3 %). This allowed a comparison of catalytic performances. Following a similar procedure as used in the synthesis of the precursors **2a**$^+$ and **2b**$^+$, $[Re(\eta^6\text{-}C_6H_5)_2]^+$ was lithiated with LDA and subsequently quenched with 2,2′-bipyridine which led to $[Re(\eta^6\text{-}C_6H_5\text{-}(C_{10}H_7N_2))(\eta^6\text{-}C_6H_6)]^+$ (**5a**$^+$) and $[Re(\eta^6\text{-}C_6H_5\text{-}(C_{10}H_7N_2))_2]^+$ (**5b**$^+$) (*Scheme 3* and *Supporting Information*). Complex **5a**$^+$ was then reacted with $[Ru(CO)_2Cl_2]_n$ to give $[Re(\eta^6\text{-}C_6H_5\text{-}(Ru(bpy)(CO)_2Cl_2)(\eta^6\text{-}C_6H_6)]^+$ (**6a**$^+$). This complex was purified by preparative HPLC. Most $[Re(\eta^6\text{-}C_6H_5)_2]^+$-type complexes have

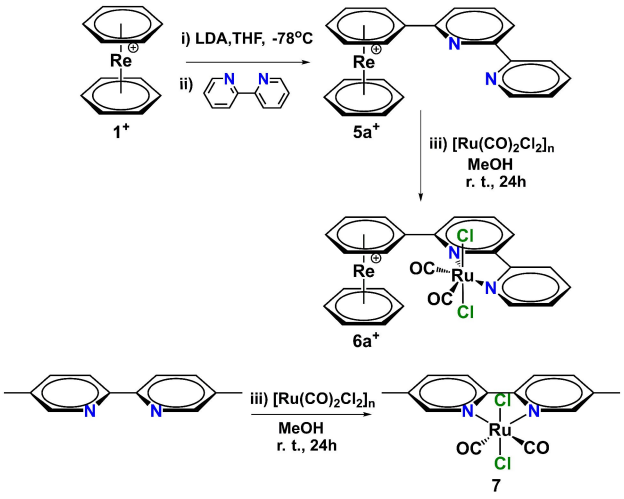

Scheme 3. Reaction scheme for the conjugation of 2,2′-bipyridine electronically connected to $[Re(\eta^6\text{-}C_6H_6)_2]^+$. Reaction conditions: i) lithiation/deprotonation 1.5–2.5 equiv. of LDA, 1.5 h, −78 °C, THF. ii) *In situ* electrophilic attack 5 h, −78 °C, THF; electrophile: 2,2′-bipyridine. iii) Complexation, $[Ru(CO)_2Cl_2]_n$ as precursor, 1 d, r.t.

a typical yellow color but **4a**$^+$, **4b**$^+$ and **6**$^+$ are orange. Due to their positive charges, they are water soluble to some extent. As a standard, we also prepared the already known catalyst trans(Cl)-[Ru(dmbpy)$(CO)_2Cl_2$] (**7**) according to the previously reported procedure.[52]

Photocatalytic CO_2 Reduction

Photocatalysis experiments were performed for the three different catalysts **4a**$^+$, **4b**$^+$ and **6a**$^+$, and complex **7** as reference. All catalysts are inactive in the absence of photosensitizer (PS) and/or sacrificial electron donor (SED). Photocatalysis requires a multicomponent system where a photosensitizer, ([Ru$(bpy)_3]Cl_2$ in our experiments), is employed to harvest the light energy and an electron donor is irreversible oxidized (*Scheme S1*). After excitation of the [Ru$(bpy)_3]^{2+}$, a reductive quenching of the excited state takes place by reductive quenching by the sacrificial electron donor (BNAH). This process is followed by electron transfers steps to the catalysts and subsequent reduction of CO_2 to CO. Photocatalytic CO_2 reduction was carried out in 10 mL CO_2-saturated DMF/H_2O (9:1 *v/v*) solution containing 0.5 mM [Ru$(bpy)_3]Cl_2$ as photosensitizer (PS), 0.1 M 1-benzyl-1,4-dihydronicotinamide (BNAH) as sacrificial electron donor. Catalysis was performed at three different catalyst concentrations (1 μM, 5 μM and 10 μM, based on Ru).

BNAH as sacrificial electron donor has been studied in detail in combination with $[Ru(bpy)_3]Cl_2$ as PS.[22,52,53] The results showed that BNAH acts as a one-electron donor producing the dimer 1,1′-dibenzyl-1,1′,4,4′-tetrahydro-4,4′-binicotinamide (BNA_2) as product of the reductive quenching process.[22,25,53,54] The 10% water content was selected following the work by *Ishida* and co-workers. They found that this concentration gives the highest amount of reduction products.[22] The water in the solution plays a role as proton donor/shuttle, but an excessive amount decreases the reductive quenching efficiency of [Ru$(bpy)_3]Cl_2$ with BNAH.[22,53] The solutions containing the catalysts were irradiated for 6 h from the bottom with a LED lamp (470 nm, photon flux of 0.18 ± 0.02 μE/s). The gaseous products were analyzed by gas chromatography (GC). Under these conditions, only CO and no H_2 was detected as a gaseous product together with about 5–10 mol-% formate relative to CO, quantified by NMR spectroscopy with dimethylmalonic acid standard (quantitative NMR quality) as a reference. The absence of H_2 in the headspace under the experimental conditions suggested that the reduced catalyst reacts only or at least preferably with CO_2 rather than with H^+.

Figure 2 shows the time-courses of the photocatalytic CO_2 reduction as well as calculated TOFs for 1 μM catalyst (*Figures S1–S4* show 5 and 10 μM). To properly compare the performance of the different catalysts, we emphasize that the concentrations are calculated and indicated as 'concentrations of Ru atoms'. For example, when comparing the results of catalysis at 5 μM, the concentration of **4b**$^+$ is only 2.5 μM. For catalysts **4a**$^+$, **4b**$^+$ and **7**, the rate of CO formation increases rapidly with time, reaching a maximum after around 30 min. After that point, the CO_2 reduction rate decreases, and catalysis ceases a few hours later. This effect is most obvious at higher concentrations. For example, CO formation stops almost completely after 3 h when photocatalysis is performed at 5 or 10 μM in Ru. This phenomenon has been previously observed by *Ishida* and co-workers in similar, Ru-based mononuclear complexes, and was attributed to a decrease in the concentration of the electron donor (BNAH), and a simultaneous increase of its oxidation product BNA_2.[53] The latter quenches the excited state of the photosensitizer (PS*) faster than BNAH, thereby affecting the photochemical CO_2 reduction.[54] About 13% of BNAH is used up at the end of photocatalysis at 10 μM in Ru. Since bubbling of

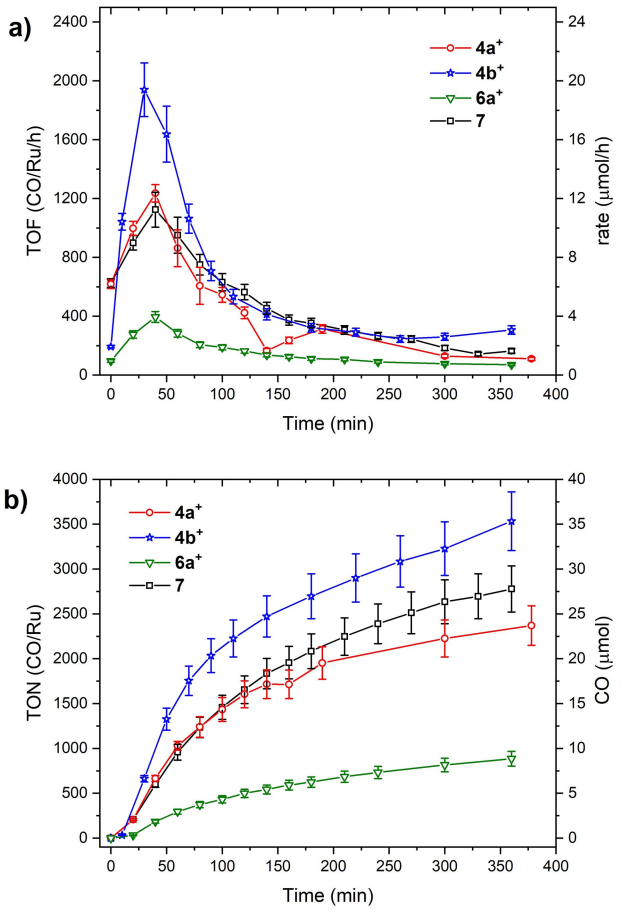

Figure 2. Comparison in TOF (a) and TON (b) as a function of time for **4a**$^+$, **4b**$^+$, **6a**$^+$ and **7** at 1 μM [Ru]. Experimental conditions: 10 mL CO_2-saturated solution DMF/H_2O (9:1 *v/v*), 500 μM $[Ru(bpy)_3]Cl_2$, 0.1 M BNAH, 470 nm LED (photon flux of 0.18 ± 0.02 μE/s).

CO_2 was not continuous during the photocatalysis experiments, the decrease in CO_2 concentration in solution could contribute additionally to slow down the rate of catalysis.

Complexes **4a**$^+$, **4b**$^+$ and **7** all show a better performance than catalyst **6a**$^+$, probably due to an increase of steric effects induced by the rhenium sandwich. The pendent catalytic unit in **6a**$^+$ has some degrees of structural freedom around the C–C bond (sandwich-bpy), as indicated by NMR data, but the $[Re(\eta^6\text{-}C_6H_5)_2]^+$ unit is still quite bulky and might affect the CO_2 coordination to Ru. Additionally, the electron withdrawing effect of the coupled sandwich unit causes an electronic deficiency on the Ru atom making it less likely to attach a CO_2 molecule. The dominant factor amongst these is difficult to assess, and most likely a combination of both is responsible for the decrease in performance.

Quantum yields were calculated from the maximum rate of CO_2 to CO conversion and the number of incident photons. Two photons are required to reduce one CO_2 molecule. The quantum yields are between 1.2 % and 13.5 %, reaching a maximum for catalyst **4b**$^+$ at 5 μM. The comparison of photocatalysis at different concentrations is a way to approach rate-limiting steps. With photocatalysis at concentrations of 5 or 10 μM, the catalytic performances (TONs and TOFs) of **4a**$^+$, **4b**$^+$, and **7** are essentially the same (*Figure 3*), regardless if one or two catalysts are conjugated to the $[Re(\eta^6\text{-arene})_2]^+$ framework, or if the catalyst is not derivatized at all. This situation changes at 1 μM concentrations, where the dinuclear catalyst **4b**$^+$ becomes superior in TONs but even more distinct in TOFs as compared to the two other

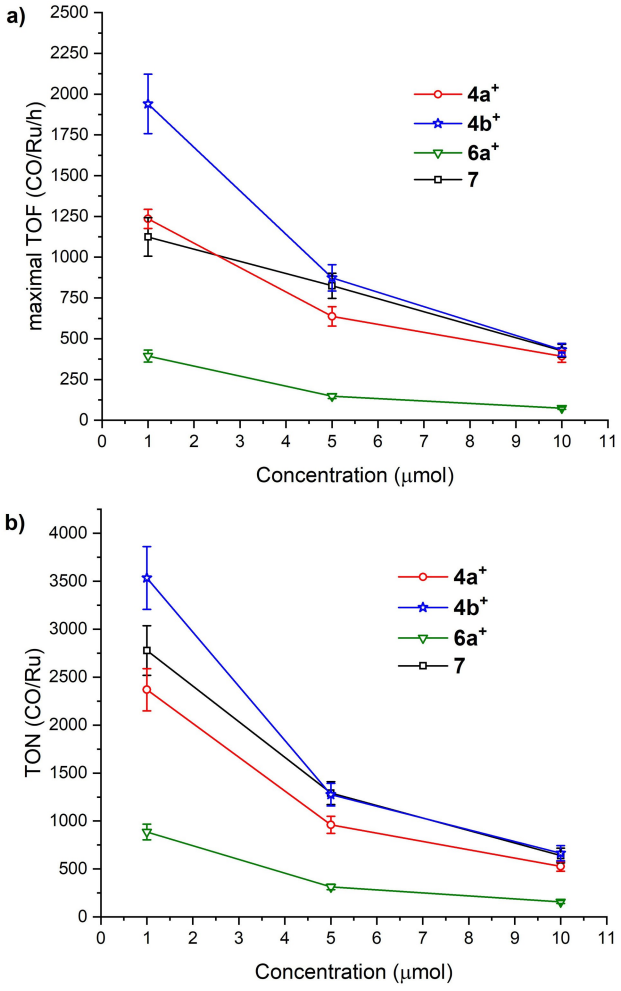

Figure 3. TONs and maximum TOFs for CO_2 reduction vs. catalyst concentrations at a constant photon flux of 0.18 ± 0.02 μE/s. Experimental conditions: 10 mL DMF/water 9:1, 500 μM $[Ru(bpy)_3]Cl_2$, 0.1 M BNAH, 470 nm LED irradiation.

catalysts. The data indicates that in the 5 to 10 μM concentration range, the catalytic cycle is regulated by the photochemical process, that is, CO_2 reduction is faster than the delivery of a second electron to an already singly reduced complex. Indeed, as shown in *Figure 3* and *Table S1*, the maximum TOF for the conversion CO_2 to CO decreases when the catalyst concentration increases, but the absolute rate of CO_2 formation remains about constant. This implies a limitation by the photocycle. Lowering the concentrations of catalysts reveals substantial differences in catalysis for **4a**$^+$, **4b**$^+$ and **7**. Catalyst **4b**$^+$ becomes significantly more active than **4a**$^+$ and **7** at 1 μM (based on Ru). An increase by almost a factor of two was achieved when **4b**$^+$ is compared to **4a**$^+$ and **7**. In addition, this also leads to an increase of the TONs following the series **4b**$^+$ > **7** > **4a**$^+$. After about 100 min into catalysis, the CO_2 reduction rate for **4b**$^+$ approaches those of **4a**$^+$ and **7**. Faster accumulation of BNA_2, which quenches the photocycle might be responsible for this observation. If the number of electrons were not limiting, a much greater difference would be expected as is actually found in electrocatalysis (*vide infra*). The results as obtained at low concentrations point to a cooperative effect between the two catalytic subunits in **4b**$^+$ under these conditions.

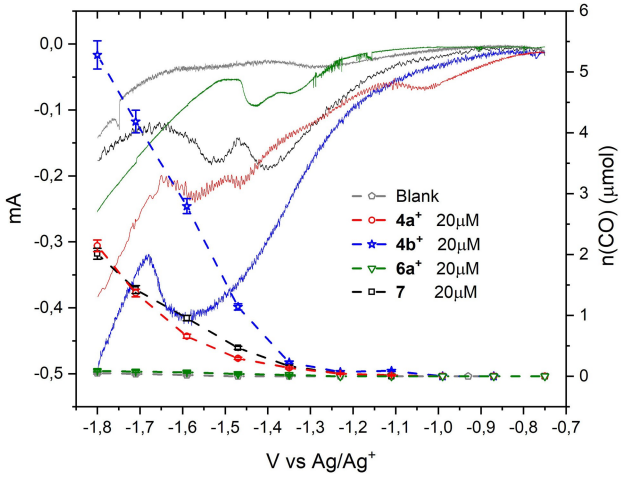

Figure 4. LSV experiments of **4a**$^+$, **4b**$^+$, **6a**$^+$ and **7**. Solid lines: current, dashed lines: amount of CO produced. Conditions: 20 μM ruthenium, 1 mM [TBA]PF_6 as electrolyte, DMF/H_2O (9:1), applied potential: −0.75 V to −1.80 V *vs.* Ag/Ag$^+$, WE = Hg pool, CE = Pt, RE = Ag/AgCl, GC/TCD quantification of CO production.

Electrocatalytic CO_2 Reduction

Electrocatalytic experiments were performed with catalysts **4a**$^+$, **4b**$^+$, **6a**$^+$ and **7** to complement the photocatalytic results and to exclude the influence of the photochemical cycle. The three-compartment cell consisted of a Hg pool working electrode, a Pt wire as auxiliary and Ag/AgCl as a reference electrode (*Figure S5*). Linear sweep voltammetry (LSV) was performed with CO_2 saturated DMF/H_2O (9:1) solutions containing 20 μM total ruthenium at a low scan rate (0.1 mV/s) (*Figures 4* and *S6*). Samples from the headspace of the cell were taken every 20 min (equivalent to 120 mV steps). For the catalysts **4a**$^+$, **4b**$^+$ and **7**, the increase in current correlates well with CO formation. GC analyses of **4a**$^+$ and **4b**$^+$ showed that CO_2 reduction slowly starts at potentials more negative than −1.1 V. For reference complex **7**, the detection of CO is observed only below −1.2 V *vs.* Ag/AgCl. The amount of CO formed with **4b**$^+$ is approximately double of what is obtained for **4a**$^+$ or **7**, demonstrating its higher electrocatalytic activity (based on Ru). The *Faradaic* efficiency (FE) for CO over the full scan region ranges from 45% for **4a**$^+$ to 75% for **4b**$^+$. For all catalysts, a considerable part of the overall current does not account for the formation of CO but rather H_2 (see *Table S2*), and likely for some formate or any other unidentified reduction products. *Figure S6* and *Table S2* show indeed, that below −1.5 V *vs.* Ag/AgCl, significant amounts of H_2 are produced together with CO. Apparently, different catalytic domains exist, and at strongly negative potentials, an alternative mechanism for the reduction of H^+ into H_2 competes with the reduction of CO_2 to CO.

Complex **6a**$^+$ behaves very differently: it shows about the same activity as the blank experiment using only the Hg pool electrode and no catalyst. Catalyst **6a**$^+$ is thus considered electrocatalytically inactive and the entire CO comes from the activity of the electrode itself (*Figures 4* and *S6*, *Table S2*). We note in particular that the two mononuclear catalysts **4a**$^+$ and **7** have an essentially identical behavior whereas the dinuclear complex **4b**$^+$ displays an activity superior to these two complexes, much in line with our observations from photocatalysis. Moreover, given the redox potential of −1.3 V *vs.* Ag/AgCl for $[Ru(bipy)_3]^{2+/+}$ in DMF,[55] and the lack of H_2 in photocatalysis, we note that the mechanism of CO formation at the mild potential of −1.2 V *vs.* Ag/AgCl should be the relevant one for photocatalysis.

To further elaborate on the mechanism at mild potentials, controlled potential electrolysis (CPE) was performed at −1.2 V *vs.* Ag/AgCl. This potential is similar to the reduction potential of the photosensi-

tizer in photocatalysis. Therefore, comparisons between photo- and electrocatalysis are more meaningful. GC Analyses evidence that **4b**$^+$ produces significantly more CO than all other catalysts and maintains a high catalytic activity over a period of 18 h (*Figure 5* and *S7*). It produces almost twice the amount of CO as compared to **7** at equal Ru concentrations. The difference to **4a**$^+$ is even larger, reaching about three times the amount. Catalyst **4b**$^+$ achieves 165 ± 7 TONs which is very high for the applied potential of −1.2 V *vs.* Ag/AgCl.[4] We emphasize that no H_2 was detected at this potential for any of the catalysts or the blank (detection limit 0.30 ± 0.02 μmol). These results are in agreement with photocatalysis where no H_2 evolution was observed. Consequently, similar mechanisms could operate for the photo- and electrocatalysis under these particular conditions. The FE for **4b**$^+$ at −1.2 V *vs.* Ag/AgCl is up to 98%, underlining the selectivity of this catalyst for CO formation. In **4a**$^+$ and **7**, the *Faradaic* efficiencies only reach values close to 85% and 91%, respectively. The 'missing' electrons are most probably associated with the formation of HCOOH instead of CO. These results underline the superiority of the multi-nuclear catalyst **4b**$^+$ over the mononuclear analogues **4a**$^+$ and **7**. *Table S3* summarizes the products obtained and the *Faradaic* efficiencies for all catalysts. Comparing with literature values is difficult since conditions such as potential, solvent, concentration of catalyst, etc. are often different. For catalysts of the type [Ru(L)(CO)$_2$Cl(X)] with L = bpy, mesbpy and X = Cl, COOMe, *etc.* high selectivity for CO over HCOOH or H_2 was usually found, with maximum FE of about 95%.[14,56] With other Ru(II) catalysts such as $[Ru(bpy)_2(CO)_2]^{2+}$ or related structures, selectivities and TONs vary depending on the conditions.[57–60]

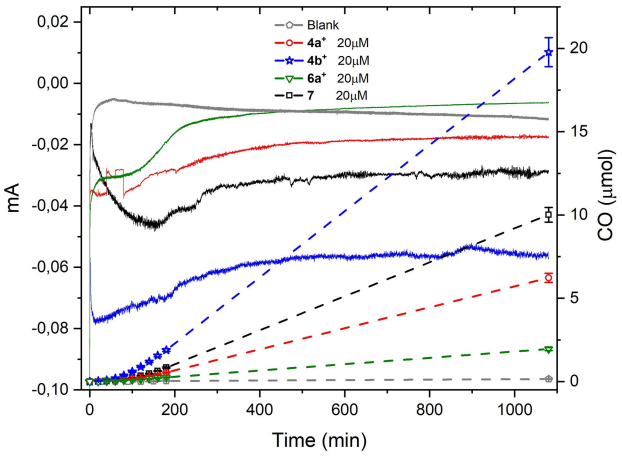

Figure 5. CPE experiments of **4a**$^+$, **4b**$^+$, **6a**$^+$ and **7** (18 h). Solid lines: current, dashed lines: amount of CO produced. Conditions: 20 μM of ruthenium, 0.1 M [TBA]PF_6 as electrolyte, DMF/H_2O (9:1), applied potential: −1.2 V *vs.* Ag/AgCl, WE = Hg pool, CE = Pt, RE = Ag/AgCl, GC/TCD quantification of CO production. No H_2 observed at this potential.

Cyclic Voltammetry and IR-SEC

Cyclic voltammetry (CV) revealed irreversible cathodic waves under N_2 atmosphere for all complexes **4a**$^+$, **4b**$^+$ and **7** (*Figure 6,a*). This has been reported previously and was extensively discussed for complexes of the type trans(Cl)-[Ru(bpy)(CO)$_2$Cl$_2$].[14,22,52]

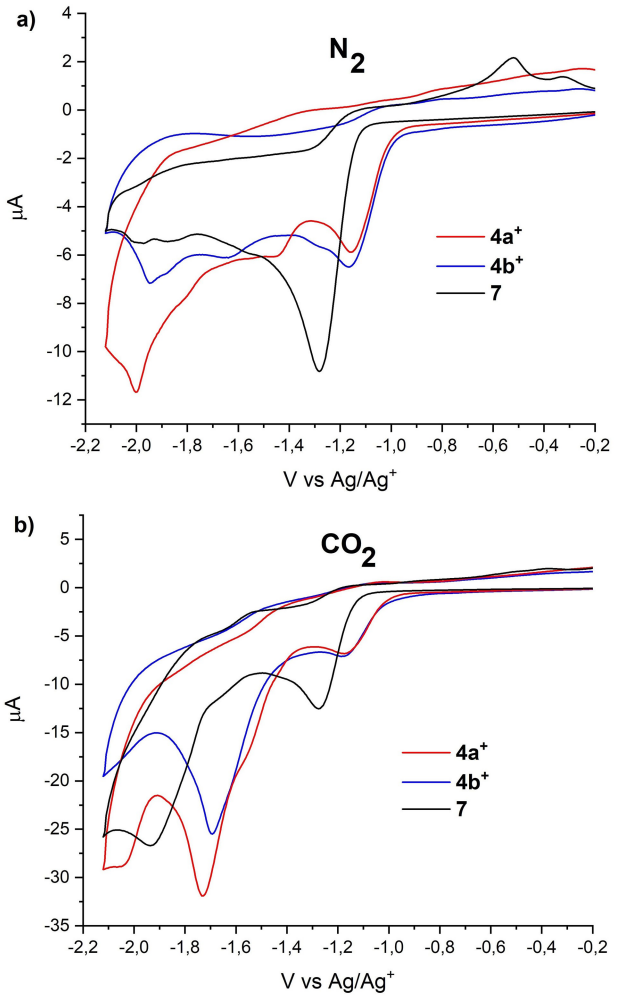

Figure 6. Comparison of cyclic voltammograms of **4a**$^+$, **4b**$^+$ and **7** in a) N_2 and b) CO_2 atmosphere. Experimental conditions: DMF, 0.1 M [TBA][PF_6] as electrolyte, glassy carbon working electrode (diameter of 3 mm), Pt counter electrode, and Ag/AgCl reference electrode. Analyte concentrations 1 mM for **4a**$^+$ and **7** and 0.5 mM for **4b**$^+$, voltage step of 6 mV, sweep rate of 0.1 V/s.

The first electron reduction is believed to be bipyridine-based followed by Cl^- loss.[14,52,61] The first irreversible reduction potentials of **4a**$^+$ and **4b**$^+$ are very similar to each other with $E_{pc} = -1.16$ V and -1.17 V *vs.* Ag/AgCl respectively. For complex **7**, the first, and also irreversible reduction takes place at a slightly more negative potential, $E_{pc} = -1.28$ V *vs.* Ag/AgCl. This difference might reflect the influence of the $[Re(\eta^6\text{-arene})_2]^+$ core; the first, ligand-based reduction is anodically shifted by the positively charged rhenium complex. Moreover, it appears as if the diffusion coefficient for the functionalized catalysts is lower as compared to the reference catalyst **7** by about 40%.

For **4b**$^+$, a second reduction at -1.28 V (*vs.* Ag/AgCl) is observed, very close to the first reduction. This observation suggests that the two Ru subunits are interacting with each other, and therefore the reduction of the first Ru^{II} influences the potential of the second one. If both metal centers were electronically decoupled, only a single wave would be visible at the same potential as for **4a**$^+$. It is noteworthy that this second reduction for **4b**$^+$ occurs at the same potential as in **7**. Assuming that the first reduction balances to some extent the electron deficiency of the Re(I) center, the reduction of the second Ru^{II} will take place at the potential where the isolated reference **7** is found (-1.28 V *vs.* Ag/AgCl). The second reduction to formally produce a Ru^0 species (third in case of **4b**$^+$) differed between all catalysts, -1.44 V for **4a**$^+$, -1.64 V for **4b**$^+$ and -1.56 V **7** (*vs.* Ag/AgCl). Additional reduction processes occur at more negative potentials, especially for **4a**$^+$ and **4b**$^+$ (*Figure 4,a*). These processes are probably associated with further reductions of the ligand and/or the $Re^{I/0}$ couple, which are found at potentials close to -2.0 V (*vs.* Ag/AgCl).[45,47–49]

In a CO_2 saturated solution all three complexes exhibit a cathodic current increase at sufficiently negative potentials, indicating that they reduce CO_2 (*Figure 6,b*). For catalysts **4a**$^+$ and **7**, the first electron-reduction is shifted towards slightly more negative potentials accompanied by a small current increase as compared to N_2 saturation experiments, which is indicative for a step associated with the binding of CO_2 (*Figure 7* and *Electronic Supplementary Material*). No changes in the first electron-reduction are observed for **4b**$^+$ though. With 5% of water and catalyst **4b**$^+$, the first reduction in presence of CO_2 takes place at the same potential and with the same current intensity as under N_2 atmosphere, indicating a non-CO_2 binding step during the first electron reduction.

The differences are much more pronounced for the second reduction wave (third for **4b**$^+$) where current increases with the concentration of H_2O for all three catalysts in the CO_2 saturated solution (*Figure 7*). This process occurs at more positive potentials for **4a**$^+$ and **4b**$^+$ as compared to **7** (-1.48 V and -1.46 V as compared to -1.64 V *vs.* Ag/AgCl, respectively, for $I_c = 15\ \mu A$). It is noteworthy that in photocatalysis all electrons are supplied by the photosensitizer $[Ru(bpy)_3]^{2+}$ with a reduction potential in DMF of only -1.3 V *vs.* Ag/AgCl.[55] Therefore, this latter process, at the strongly reducing potentials, where a formal Ru^0 is formed, is not relevant either for photocatalysis nor for the CPE at -1.2 V *vs.* Ag/AgCl. In the case of **4b**$^+$, the catalytic onset occurs right after the second reduction and therefore no Ru^0 intermediate is observed. The Ru^I-{Re}-Ru^I species formed at -1.28 V *vs.* Ag/AgCl must then be the key compound in the CO_2 reduction mechanism of **4b**$^+$.

Infrared spectroelectrochemistry (IR-SEC) experiments were performed to monitor the changes in the IR bands and to identify eventual intermediates during electrocatalytic CO_2 reduction. With 0.3 M $[TBA]PF_6$ in dry DMF as electrolyte and 5 mM of **4b**$^+$, two IR vibrations are present at 1995 and 2059 cm^{-1} at resting potentials (*Figure 8*). These IR stretching frequencies are consistent with other studies of similar $[RuCl_2(CO)_2$diimine]-type complexes and with DFT calculations.[14] When the applied potential of the cell is decreased to -1.24 V in absence of CO_2, the intensities of the two bands decrease and new bands appear. The bands at 1939 and 2016 cm^{-1}, detected already at -1.19 V, have been previously described by *Kubiak et al.* and were assigned to a species of the $[RuCl(dmbpy)(CO)_2(solv)]^0$ type. This species results from a one electron reduction and subsequent Cl^- loss. This assignment agrees with our CV experiments, which show irreversible reductions at this potential. In addition to these two main IR bands, several extra bands at around 1892, 1916 and 1973 cm^{-1} emerge at this potential. Those bands most likely corresponded to species before Cl^- dissociation and solvent coordination. The vibration frequencies calculated for the five-coordinate intermediate $[RuCl(dmbpy)(CO)_2]^0$ (DFT: 1915, 1992 cm^{-1}) before DMF coordinates to the metal center, match well with the experimentally found bands (*Table S4*).

At -1.24 V *vs.* Ag/AgCl, the bands corresponding to the resting potential of **4b**$^+$ (1995 and 2059 cm^{-1}) are still observed with relatively strong intensity. This is in line with our previous assignment for a one electron reduction of **4b**$^+$ giving a mixed valence

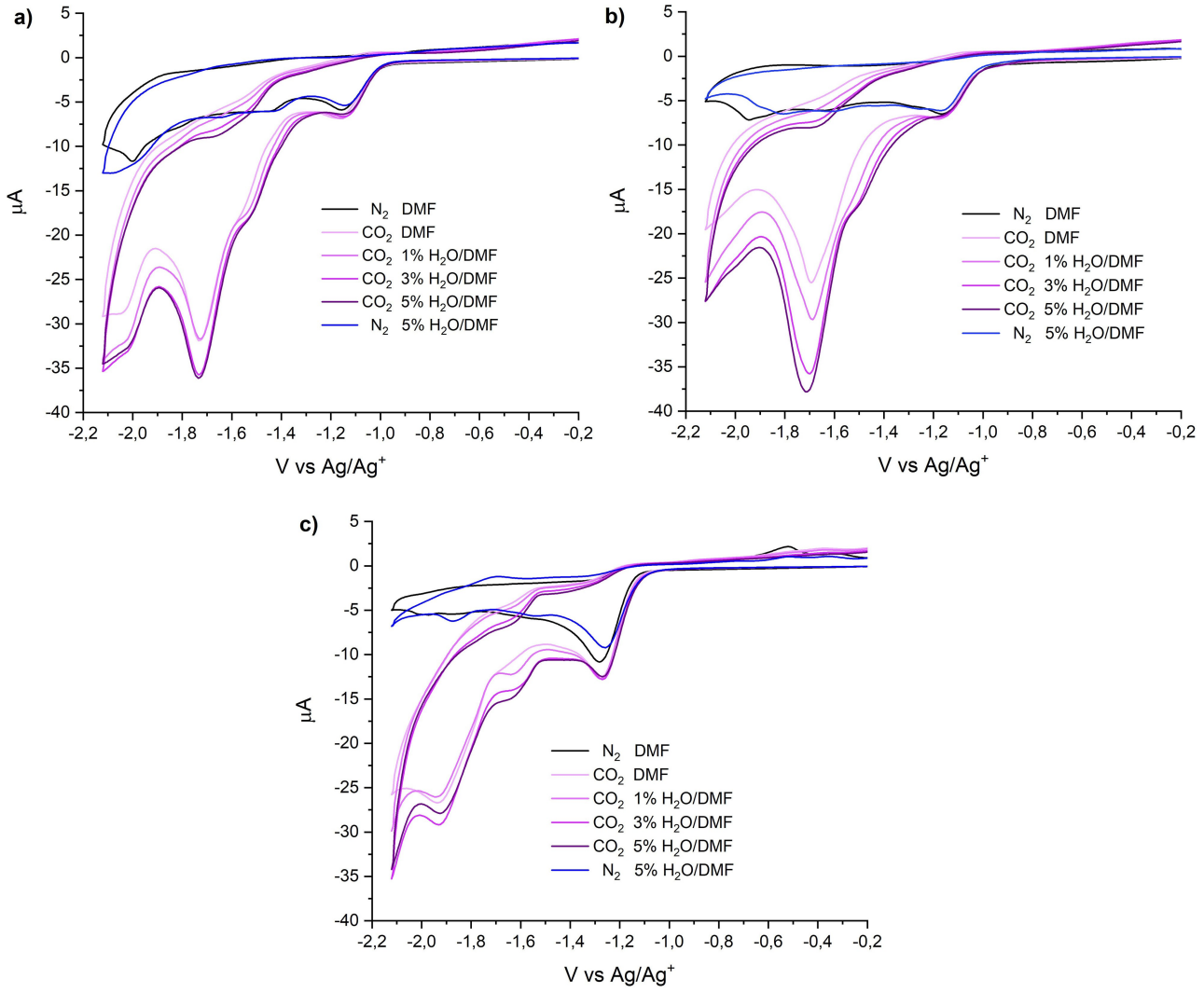

Figure 7. Cyclic voltammograms of a) **4a**$^+$, b) **4b**$^+$ and c) **7** in DMF, 0.1 M [TBA][PF_6] as electrolyte, glassy carbon working electrode (diameter of 3 mm), Pt counter electrode, and Ag/AgCl reference electrode. Analyte concentrations of 1 mM, voltage step of 6 mV, sweep rate 0.1 V/s.

compound (formal Ru^{I}-{Re}-Ru^{II}), where the second reduction (to formal Ru^{I}-{Re}-Ru^{I}) requires a slightly more negative potential. Repeating the same experiments with **4b**$^+$ but under a CO_2 atmosphere shows a very similar picture as in the absence of CO_2 at potentials down to −1.34 V *vs.* Ag/AgCl (*Figures 8*). Accordingly, CO_2 reduction catalysis is already happening at this potential, indicating that CO_2 enters the catalytic cycle after the Ru^{I}-{Re}-Ru^{I} species is formed, and reacts with this species directly. In addition, there is no evidence for the formation of any formal Ru^{II}-{Re}-$Ru^{II}(CO)_3$ or any other Ru^{II}-COO-Ru^{II} related species as a long-lasting intermediate or present in significant concentrations. Once CO_2 is coordinated, the catalytic process is fast.

Based on these experiments and the observed synergism in **4b**$^+$, the following mechanism is proposed (*Scheme 4*); complex **4b**$^+$ (**Ru^{II}-{Re}-Ru^{II}**) is first reduced to the intermediate $[\{Ru^{II}\}Cl_2]$-{Re}-$[\{Ru^{I}\}Cl_2\}]^0$ ({Ru} = [Ru(dmbpy)$(CO)_2$], {Re} = [Re(η^6-C_6H_6)$_2$]$^+$). This complex loses irreversibly one Cl^-. The complex $[\{Ru^{II}Cl_2\}$-{Re}-$\{Ru^{I}Cl\}]^+$ is an important intermediate according to literature[14] to which a solvent coordinates to form $[\{Ru^{II}Cl_2\}$-{Re}-$\{Ru^{I}\}$(DMF)Cl$\}]^+$ (**Ru^{II}-{Re}-Ru^{I}**). A second reduction/substitution follows and $[\{Ru^{I}\}$(DMF)Cl)-{Re}-$\{Ru^{I}\}$(DMF)Cl$\}]^+$ (**Ru^{I}-{Re}-Ru^{I}**) forms. At this point, CO_2 can be activated by the **Ru^{I}-{Re}-Ru^{I}** intermediate, forming a Ru^{II}-COO-Ru^{II} species in which one metal center serves as a *Lewis* base coordinating the CO_2 through the carbon atom and

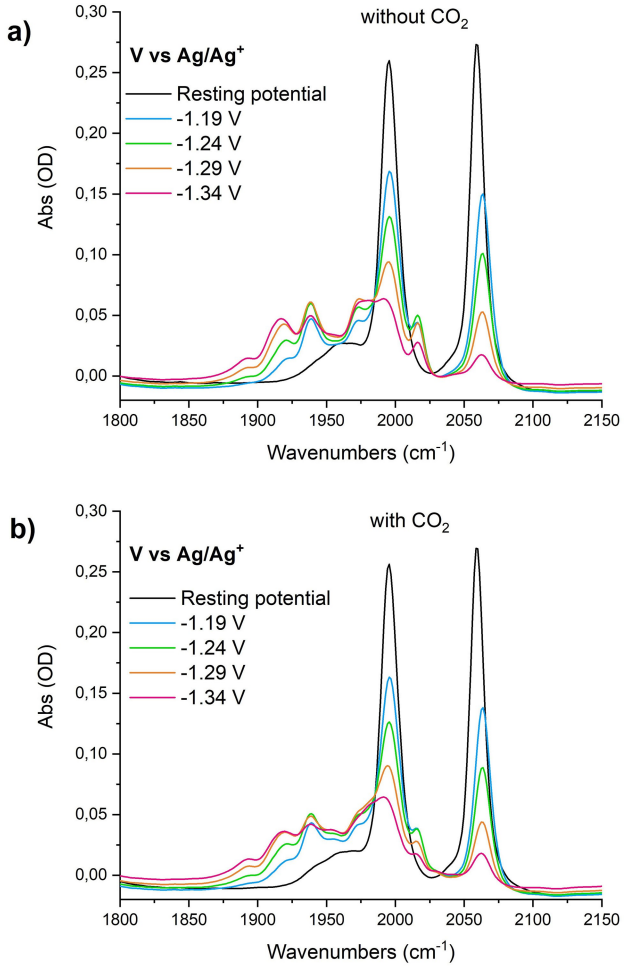

Figure 8. IR-SEC spectra of complex **4b**$^{+}$ in solution at selected potentials *vs.* Ag/AgCl in a) absence of CO_2 and b) in presence of CO_2. Conditions: 5 mM of **4b**$^{+}$; 0.3 M $TBAPF_6$/DMF; Pt working electrode, Pt counter electrode, Ag wire reference electrode.

the other metal center serves as a *Lewis* acid binding the CO_2 at the oxygen. This type of push-pull interaction has previously been observed to facilitate the CO_2 to CO reduction and produce synergistic effects on other dinuclear catalysts.[28,31,35] This key step happens due to the structural degrees of freedom of the scaffold. Subsequently, the CO_2 adduct complex is protonated to release H_2O and produce the tricarbonyl complex $[\{Ru^{II}\}(DMF)Cl\}\text{-Re-}\{Ru^{II}\}(CO)(Cl)\}]^{3+}$ (**Ru^{II}-{Re}-Ru^{II}-CO**) from which CO is released and the **Ru^{II}-{Re}-Ru^{II}** is reformed and re-enters the catalytic cycle.

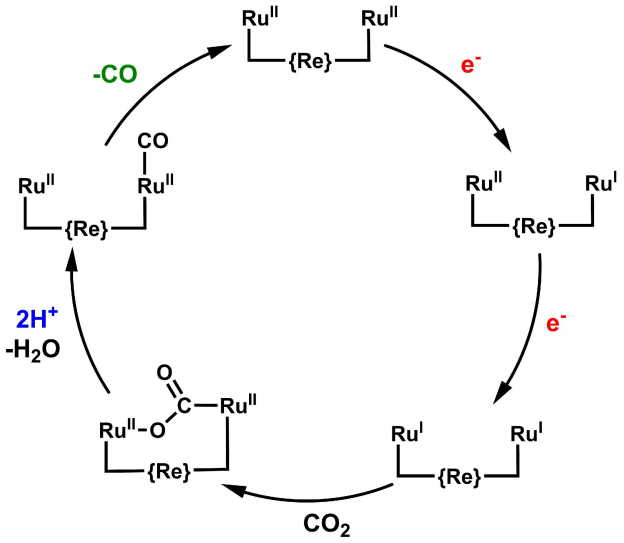

Scheme 4. Proposed mechanisms for the reduction of CO_2 to CO and H_2O through a synergistic pathway between the two catalytic subunits in **4b**$^{+}$. All reductions and protonations are formally drawn as metal-based but can involve the ligand as well.

Conclusions

A series of novel complexes with a $[Re(\eta^6\text{-arene})_2]^{+}$ core, conjugated to one or two $[Ru(dmbpy)(CO)_2Cl_2]$ complexes as catalytic subunits have been synthesized and fully characterized. The photo- and electrocatalytic performance, as well as electrochemical and spectroscopic properties, were studied in detail. Kinetic enhancement in photo- and electrocatalytic activities were observed for complexes comprising two catalysts as compared with mono-conjugation or free catalyst. The doubly conjugated catalyst also showed a stable electrocatalytic performance for CO_2 reduction over 18 h with a significant increase in TONs as compared to the monomeric structures. The improvement in catalytic activities found for the di-functionalized system implies a synergistic mechanism in which one functionality serves as a Lewis base while the second one is a Lewis acid. The proposed mechanism is supported by electrochemistry, spectroelectrochemistry and DFT studies.

The stability and the structural flexibility of $[Re(\eta^6\text{-}C_6H_5R)_2]^{+}$ together with the improvement in photo- and electrocatalytic activity support our hypothesis that the $[Re(C_6H_5R)_2]^{+}$ frameworks are suitable for many other purposes in which harsh conditions such as light irradiation or electrochemistry are involved. We emphasize that the approach presented goes beyond these examples and is adaptable to many

other directions in catalysis. Conjugation of other types of functionalities such as proton shuttles or photosensitizers together with catalysts could lead to other synergistic effects. Furthermore, the results of this work provides new insights regarding the development of supramolecular complexes where multiple functionalities can be combined together in one single architecture.

Acknowledgements

Financial support from the Swiss National Science Foundation (SNSF) under the Swiss South Africa Joint Research Project IZLSZ2_170856 is gratefully acknowledged.

Author Contribution Statement

Daniel Hernández-Valdés did the synthetic and catalytic studies and wrote the paper, *Ricardo Fernández-Terán* performed the time-resolved IR experiments, *Benjamin Probst* contributed the analyzing tools, *Bernhard Spingler* did the X-ray crystallography and *Roger Alberto* designed the project.

References

[1] V. Balzani, A. Credi, M. Venturi, 'Photochemical Conversion of Solar Energy', *ChemSusChem* **2008**, *1*, 26 – 58.

[2] S. Chu, A. Majumdar, 'Opportunities and challenges for a sustainable energy future', *Nature* **2012**, *488*, 294 – 303.

[3] M. Cokoja, C. Bruckmeier, B. Rieger, W. A. Herrmann, F. E. Kühn, 'Transformation of Carbon Dioxide with Homogeneous Transition-Metal Catalysts: A Molecular Solution to a Global Challenge?', *Angew. Chem. Int. Ed.* **2011**, *50*, 8510 – 8537; *Angew. Chem.* **2011**, *123*, 8662 – 8690.

[4] K. E. Dalle, J. Warnan, J. J. Leung, B. Reuillard, I. S. Karmel, E. Reisner, 'Electro- and Solar-Driven Fuel Synthesis with First Row Transition Metal Complexes', *Chem. Rev.* **2019**, *119*, 2752 – 2875.

[5] M. Schreier, L. Curvat, F. Giordano, L. Steier, A. Abate, S. M. Zakeeruddin, J. Luo, M. T. Mayer, M. Grätzel, 'Efficient photosynthesis of carbon monoxide from CO_2 using perovskite photovoltaics', *Nat. Commun.* **2015**, *6*, 7326.

[6] M. Schreier, F. Héroguel, L. Steier, S. Ahmad, J. S. Luterbacher, M. T. Mayer, J. Luo, M. Grätzel, 'Solar conversion of CO_2 to CO using Earth-abundant electrocatalysts prepared by atomic layer modification of CuO', *Nat. Energy* **2017**, *2*, 17087.

[7] K. R. Thampi, J. Kiwi, M. Graetzel, 'Methanation and photomethanation of carbon dioxide at room temperature and atmospheric pressure', *Nature* **1987**, *327*, 506 – 508.

[8] J. Hawecker, J.-M. Lehn, R. Ziessel, 'Electrocatalytic reduction of carbon dioxide mediated by $Re(bipy)(CO)_3Cl$ (bipy = 2,2′-bipyridine)', *J. Chem. Soc. Chem. Commun.* **1984**, 328 – 330.

[9] M. Beley, J.-P. Collin, R. Ruppert, J.-P. Sauvage, 'Nickel(II)-cyclam: an extremely selective electrocatalyst for reduction of CO_2 in water', *J. Chem. Soc. Chem. Commun.* **1984**, 1315 – 1316.

[10] B. J. Fisher, R. Eisenberg, 'Electrocatalytic reduction of carbon dioxide by using macrocycles of nickel and cobalt', *J. Am. Chem. Soc.* **1980**, *102*, 7361 – 7363.

[11] A. J. Morris, G. J. Meyer, E. Fujita, 'Molecular Approaches to the Photocatalytic Reduction of Carbon Dioxide for Solar Fuels', *Acc. Chem. Res.* **2009**, *42*, 1983 – 1994.

[12] H. Shirley, X. Su, H. Sanjanwala, K. Talukdar, J. W. Jurss, J. H. Delcamp, 'Durable Solar-Powered Systems with Ni-Catalysts for Conversion of CO_2 or CO to CH_4', *J. Am. Chem. Soc.* **2019**, *141*, 6617 – 6622.

[13] F. Yoshitomi, K. Sekizawa, K. Maeda, O. Ishitani, 'Selective Formic Acid Production via CO_2 Reduction with Visible Light Using a Hybrid of a Perovskite Tantalum Oxynitride and a Binuclear Ruthenium(II) Complex', *ACS Appl. Mater. Interfaces* **2015**, *7*, 13092 – 13097.

[14] C. W. Machan, M. D. Sampson, C. P. Kubiak, 'A Molecular Ruthenium Electrocatalyst for the Reduction of Carbon Dioxide to CO and Formate', *J. Am. Chem. Soc.* **2015**, *137*, 8564 – 8571.

[15] M. D. Sampson, A. D. Nguyen, K. A. Grice, C. E. Moore, A. L. Rheingold, C. P. Kubiak, 'Manganese Catalysts with Bulky Bipyridine Ligands for the Electrocatalytic Reduction of Carbon Dioxide: Eliminating Dimerization and Altering Catalysis', *J. Am. Chem. Soc.* **2014**, *136*, 5460 – 5471.

[16] H. Rao, L. C. Schmidt, J. Bonin, M. Robert, 'Visible-light-driven methane formation from CO_2 with a molecular iron catalyst', *Nature* **2017**, *548*, 74 – 77.

[17] G. F. Manbeck, E. Fujita, 'A review of iron and cobalt porphyrins, phthalocyanines and related complexes for electrochemical and photochemical reduction of carbon dioxide', *J. Porphyrins Phthalocyanines* **2015**, *19*, 45 – 64.

[18] R. Francke, B. Schille, M. Roemelt, 'Homogeneously Catalyzed Electroreduction of Carbon Dioxide – Methods, Mechanisms, and Catalysts', *Chem. Rev.* **2018**, *118*, 4631 – 4701.

[19] A. L. Ostericher, T. M. Porter, M. H. Reineke, C. P. Kubiak, 'Thermodynamic targeting of electrocatalytic CO_2 reduction: advantages, limitations, and insights for catalyst design', *Dalton Trans.* **2019**, *48*, 15841 – 15848.

[20] B. Kumar, M. Llorente, J. Froehlich, T. Dang, A. Sathrum, C. P. Kubiak, 'Photochemical and Photoelectrochemical Reduction of CO_2', *Annu. Rev. Phys. Chem.* **2012**, *63*, 541 – 569.

[21] C. D. Windle, R. N. Perutz, 'Advances in molecular photocatalytic and electrocatalytic CO_2 reduction', *Coord. Chem. Rev.* **2012**, *256*, 2562 – 2570.

[22] Y. Kuramochi, J. Itabashi, K. Fukaya, A. Enomoto, M. Yoshida, H. Ishida, 'Unexpected effect of catalyst concentration on photochemical CO_2 reduction by *trans*(Cl)–$Ru(bpy)(CO)_2Cl_2$: new mechanistic insight into the $CO/HCOO^-$ selectivity', *Chem. Sci.* **2015**, *6*, 3063 – 3074.

[23] H. Takeda, O. Ishitani, 'Development of efficient photocatalytic systems for CO_2 reduction using mononuclear

and multinuclear metal complexes based on mechanistic studies', *Coord. Chem. Rev.* **2010**, *254*, 346 – 354.

[24] B. Gholamkhass, H. Mametsuka, K. Koike, T. Tanabe, M. Furue, O. Ishitani, 'Architecture of Supramolecular Metal Complexes for Photocatalytic CO_2 Reduction: Ruthenium – Rhenium Bi- and Tetranuclear Complexes', *Inorg. Chem.* **2005**, *44*, 2326 – 2336.

[25] Y. Tamaki, T. Morimoto, K. Koike, O. Ishitani, 'Photocatalytic CO_2 reduction with high turnover frequency and selectivity of formic acid formation using Ru(II) multinuclear complexes', *Proc. Natl. Acad. Sci. USA* **2012**, *109*, 15673 – 15678.

[26] R. Kuriki, K. Sekizawa, O. Ishitani, K. Maeda, 'Visible-Light-Driven CO_2 Reduction with Carbon Nitride: Enhancing the Activity of Ruthenium Catalysts', *Angew. Chem. Int. Ed.* **2015**, *54*, 2406 – 2409; *Angew. Chem.* **2015**, *127*, 2436 – 2439.

[27] P. D. Frischmann, K. Mahata, F. Würthner, 'Powering the future of molecular artificial photosynthesis with light-harvesting metallosupramolecular dye assemblies', *Chem. Soc. Rev.* **2013**, *42*, 1847 – 1870.

[28] J.-W. Wang, D.-C. Zhong, T.-B. Lu, 'Artificial photosynthesis: Catalytic water oxidation and CO_2 reduction by dinuclear non-noble-metal molecular catalysts', *Coord. Chem. Rev.* **2018**, *377*, 225 – 236.

[29] J. Lan, T. Liao, T. Zhang, L. W. Chung, 'Reaction Mechanism of Cu(I)-Mediated Reductive CO_2 Coupling for the Selective Formation of Oxalate: Cooperative CO_2 Reduction To Give Mixed-Valence $Cu_2(CO_2)^{\bullet-}$ and Nucleophilic-Like Attack', *Inorg. Chem.* **2017**, *56*, 6809 – 6819.

[30] R. Angamuthu, P. Byers, M. Lutz, A. L. Spek, E. Bouwman, 'Electrocatalytic CO_2 Conversion to Oxalate by a Copper Complex', *Science* **2010**, *327*, 313 – 315.

[31] L.-M. Cao, H.-H. Huang, J.-W. Wang, D.-C. Zhong, T.-B. Lu, 'The synergistic catalysis effect within a dinuclear nickel complex for efficient and selective electrocatalytic reduction of CO_2 to CO', *Green Chem.* **2018**, *20*, 798 – 803.

[32] K. Mochizuki, S. Manaka, I. Takeda, T. Kondo, 'Synthesis and Structure of [6,6′-Bi(5,7-dimethyl-1,4,8,11-tetraazacyclotetradecane)]dinickel(II) Triflate and Its Catalytic Activity for Photochemical CO_2 Reduction', *Inorg. Chem.* **1996**, *35*, 5132 – 5136.

[33] E. A. Mohamed, Z. N. Zahran, Y. Naruta, 'Efficient electrocatalytic CO_2 reduction with a molecular cofacial iron porphyrin dimer', *Chem. Commun.* **2015**, *51*, 16900 – 16903.

[34] Z. N. Zahran, E. A. Mohamed, Y. Naruta, 'Bio-inspired cofacial Fe porphyrin dimers for efficient electrocatalytic CO_2 to CO conversion: Overpotential tuning by substituents at the porphyrin rings', *Sci. Rep.* **2016**, *6*, 24533.

[35] T. Ouyang, H.-H. Huang, J.-W. Wang, D.-C. Zhong, T.-B. Lu, 'A Dinuclear Cobalt Cryptate as a Homogeneous Photocatalyst for Highly Selective and Efficient Visible-Light Driven CO_2 Reduction to CO in CH_3CN/H_2O Solution', *Angew. Chem. Int. Ed.* **2017**, *56*, 738 – 743; *Angew. Chem.* **2017**, *129*, 756 – 761.

[36] A. Wilting, T. Stolper, R. A. Mata, I. Siewert, 'Dinuclear Rhenium Complex with a Proton Responsive Ligand as a Redox Catalyst for the Electrochemical CO_2 Reduction', *Inorg. Chem.* **2017**, *56*, 4176 – 4185.

[37] C. W. Machan, S. A. Chabolla, J. Yin, M. K. Gilson, F. A. Tezcan, C. P. Kubiak, 'Supramolecular Assembly Promotes the Electrocatalytic Reduction of Carbon Dioxide by Re(I) Bipyridine Catalysts at a Lower Overpotential', *J. Am. Chem. Soc.* **2014**, *136*, 14598 – 14607.

[38] Y. Shimazaki, T. Nagano, H. Takesue, B.-H. Ye, F. Tani, Y. Naruta, 'Characterization of a Dinuclear Mn^{V}=O Complex and Its Efficient Evolution of O_2 in the Presence of Water', *Angew. Chem. Int. Ed.* **2004**, *43*, 98 – 100; *Angew. Chem.* **2004**, *116*, 100 – 102.

[39] S. Sato, K. Koike, H. Inoue, O. Ishitani, 'Highly efficient supramolecular photocatalysts for CO_2 reduction using visible light', *Photochem. Photobiol. Sci.* **2007**, *6*, 454 – 461.

[40] M. Schulz, M. Karnahl, M. Schwalbe, J. G. Vos, 'The role of the bridging ligand in photocatalytic supramolecular assemblies for the reduction of protons and carbon dioxide', *Coord. Chem. Rev.* **2012**, *256*, 1682 – 1705.

[41] K. Koike, S. Naito, S. Sato, Y. Tamaki, O. Ishitani, 'Architecture of supramolecular metal complexes for photocatalytic CO_2 reduction: III: Effects of length of alkyl chain connecting photosensitizer to catalyst', *J. Photochem. Photobiol. A* **2009**, *207*, 109 – 114.

[42] Z.-Y. Bian, K. Sumi, M. Furue, S. Sato, K. Koike, O. Ishitani, 'A Novel Tripodal Ligand, Tris[(4′-methyl-2,2′-bipyridyl-4-yl) methyl]carbinol and Its Trinuclear Ru^{II}/Re^{I} Mixed-Metal Complexes: Synthesis, Emission Properties, and Photocatalytic CO_2 Reduction', *Inorg. Chem.* **2008**, *47*, 10801 – 10803.

[43] D. Hernández-Valdés, F. Avignon, P. Müller, G. Meola, B. Probst, T. Fox, B. Spingler, R. Alberto, '$[Re(\eta^6\text{-arene})_2]^+$ as a highly stable ferrocene-like scaffold for ligands and complexes', *Dalton Trans.* **2020**, *49*, 5250 – 5256.

[44] E. O. Fischer, A. Wirzmüller, 'Über Aromatenkomplexe von Metallen, XII. Rhenium(I)-Komplexe des Benzols und Mesitylens', *Chem. Ber.* **1957**, *90*, 1725 – 1730.

[45] M. Benz, H. Braband, P. Schmutz, J. Halter, R. Alberto, 'From Tc^{VII} to Tc^{I}; facile syntheses of bis-arene complexes $[^{99(m)}Tc(arene)_2]^+$ from pertechnetate', *Chem. Sci.* **2015**, *6*, 165 – 169.

[46] D. Hernández-Valdés, G. Meola, H. Braband, B. Spingler, R. Alberto, 'Direct Synthesis of Non-Alkyl Functionalized Bis-Arene Complexes of Rhenium and $^{99(m)}$ Technetium', *Organometallics* **2018**, *37*, 2910 – 2916.

[47] G. Meola, H. Braband, D. Hernández-Valdés, C. Gotzmann, T. Fox, B. Spingler, R. Alberto, 'A Mixed-Ring Sandwich Complex from Unexpected Ring Contraction in $[Re(\eta^6\text{-}C_6H_5Br)(\eta^6\text{-}C_6R_6)](PF_6)$', *Inorg. Chem.* **2017**, *56*, 6297 – 6301.

[48] G. Meola, H. Braband, S. Jordi, T. Fox, O. Blacque, B. Spingler, R. Alberto, 'Structure and reactivities of rhenium and technetium bis-arene sandwich complexes $[M(\eta^6\text{-arene})_2]^+$', *Dalton Trans.* **2017**, *46*, 14631 – 14637.

[49] G. Meola, H. Braband, P. Schmutz, M. Benz, B. Spingler, R. Alberto, 'Bis-Arene Complexes $[Re(\eta^6\text{-arene})_2]^+$ as Highly Stable Bioorganometallic Scaffolds', *Inorg. Chem.* **2016**, *55*, 11131 – 11139.

[50] M. Cleare, W. Griffith, 'Halogeno-carbonyl and-nitrosyl complexes of the platinum metals, and their vibrational spectra', *J. Chem. Soc. A* **1969**, 372 – 380.

[51] Q. Nadeem, G. Meola, H. Braband, R. Bolliger, O. Blacque, D. Hernández-Valdés, R. Alberto, 'To Sandwich Technetium: Highly Functionalized Bi-Arene Complexes $[^{99m}Tc(\eta^6\text{-arene})_2]^+$ Directly from Water and $[^{99m}TcO_4]^-$', *Angew. Chem. Int. Ed.* **2020**, *59*, 1197 – 1200.

[52] Y. Kuramochi, J. Itabashi, M. Toyama, H. Ishida, 'Photochemical CO_2 Reduction Catalyzed by *Trans*(Cl)-[Ru(2,2-bipyridine)$(CO)_2Cl_2$] Bearing Two Methyl Groups at 4,4-, 5,5′- or 6,6′-Positions in the Ligand', *ChemPhotoChem* **2018**, *2*, 314 – 322.

[53] Y. Kuramochi, M. Kamiya, H. Ishida, 'Photocatalytic CO_2 Reduction in *N*,*N*-Dimethylacetamide/Water as an Alternative Solvent System', *Inorg. Chem.* **2014**, *53*, 3326 – 3332.

[54] Y. Tamaki, K. Koike, T. Morimoto, O. Ishitani, 'Substantial improvement in the efficiency and durability of a photocatalyst for carbon dioxide reduction using a benzoimidazole derivative as an electron donor', *J. Catal.* **2013**, *304*, 22 – 28.

[55] E. Joliat, S. Schnidrig, B. Probst, C. Bachmann, B. Spingler, K. K. Baldridge, F. von Rohr, A. Schilling, R. Alberto, 'Cobalt complexes of tetradentate, bipyridine-based macrocycles: their structures, properties and photocatalytic proton reduction', *Dalton Trans.* **2016**, *45*, 1737 – 1745.

[56] S. Chardon-Noblat, A. Deronzier, R. Ziessel, D. Zsoldos, 'Selective Synthesis and Electrochemical Behavior of *trans* (Cl)- and *cis*(Cl)-[Ru(bpy)$(CO)_2Cl_2$] Complexes (bpy = 2,2′-Bipyridine). Comparative Studies of Their Electrocatalytic Activity toward the Reduction of Carbon Dioxide', *Inorg. Chem.* **1997**, *36*, 5384 – 5389.

[57] H. Ishida, H. Tanaka, K. Tanaka, T. Tanaka, 'Selective formation of $HCOO^-$ in the electrochemical CO_2 reduction catalysed by $[Ru(bpy)_2(CO)_2]^{2+}$ (bpy = 2,2′-bipyridine)', *J. Chem. Soc., Chem. Commun.* **1987**, 131 – 132.

[58] J. R. Pugh, M. R. M. Bruce, B. P. Sullivan, T. J. Meyer, 'Formation of a metal-hydride bond and the insertion of carbon dioxide. Key steps in the electrocatalytic reduction of carbon dioxide to formate anion', *Inorg. Chem.* **1991**, *30*, 86 – 91.

[59] H. Ishida, K. Tanaka, T. Tanaka, 'Electrochemical CO_2 reduction catalyzed by ruthenium complexes $[Ru(bpy)_2(CO)_2]^{2+}$ and $[Ru(bpy)_2(CO)Cl]^+$. Effect of pH on the formation of CO and $HCOO^-$', *Organometallics* **1987**, *6*, 181 – 186.

[60] H. Ishida, K. Fujiki, T. Ohba, K. Ohkubo, K. Tanaka, T. Terada, T. Tanaka, 'Ligand effects of ruthenium 2,2′-bipyridine and 1,10-phenanthroline complexes on the electrochemical reduction of CO_2', *J. Chem. Soc. Dalton Trans.* **1990**, 2155 – 2160.

[61] M.-N. Collomb-Dunand-Sauthier, A. Deronzier, R. Ziessel, 'Electrochemical behaviour of $[Ru^{II}(L)(CO)_2Cl_2][Ru^{II}(L)(CO)Cl_3][Me_4N]$ and $[Ru^{II}(L)(CO)_2(CH_3CN)_2][CF_3SO_3]_2$ complexes (L = 2,2′-bipyridine or 4,4′-isopropoxycarbonyl-2,2′-bipyridine)', *J. Electroanal. Chem.* **1993**, *350*, 43 – 55.

Received July 27, 2020
Accepted September 1, 2020